Indonesian Journal of Oceanography
Februari 2026, Vol 8 No 1: 36-47
ISSN: 2714-8726

Seasonal Variability of Surface Currents in Cempi Bay, NTB Based on ADCP and HYCOM Data

Muchammad Iqbal Havis[1]*, Mochamad Tri Hartanto[2], Esa Fajar Hidayat[3], Agustinus Sembiring[1], Nabil[2]

[1]Independent Researcher
Jakarta 12950, Indonesia
[2]Department of Marine Science and Technology, Faculty of Fisheries and Marine Sciences, IPB University
Jl. Agatis, Babakan, Dramaga, BogorJawa Barat 16680 Indonesia
[3]Department of Marine Science, Faculty of Fisheries and Marine Sciences, Universitas Brawijaya
Jl. Veteran, Lowokwaru, Malang, Jawa Timur 65145, Indonesia
Email: *muchammadiqbalhavis@gmail.com

Abstract

This study investigates the seasonal variability of surface currents in Cempi Bay, located on the southern coast of Sumbawa Island, Indonesia. Using Acoustic Doppler Current Profiler (ADCP), the data were collected during the Northwest Monsoon (NWM, February 2023) and Southeast Monsoon (SEM, August 2023), along with surface current data from the Hybrid Coordinate Ocean Model (HYCOM), we analyzed tidal and residual current dynamics at two observation points. Harmonic analysis revealed that during the NWM, currents at the eastern inner bay (ADCP-01) were predominantly tidal (76.83%), while in the western inner bay (ADCP-02), residual currents (52.30%) slightly exceeded tidal contributions. Conversely, during the SEM both stations experienced more balanced contributions in approximately 59% at both locations, with residual current influence increasing to 40–41%. HYCOM data depict the general direction of currents spatially well, but tend to underestimate at small scales as nearshore. The findings highlight the significant role of both tidal forces and monsoon-driven residual currents in shaping the seasonal surface current dynamics of Cempi Bay, providing a valuable baseline for oceanographic monitoring and coastal management in the region.

Keywords: Cempi Bay, surface currents, ADCP, HYCOM, tidal analysis

INTRODUCTION

The Indonesian archipelago, located within the Maritime Continent, exhibits highly complex oceanographic dynamics arising from the interaction of monsoonal wind systems, intricate bathymetry, and large-scale ocean circulation. Seasonal reversals of the Asian–Australian monsoon strongly regulate surface current variability throughout Indonesian waters, influencing the exchange of water masses between the Pacific and Indian Oceans. These processes play a fundamental role in regional climate modulation, marine ecosystem dynamics, and coastal environmental conditions. Consequently, understanding seasonal surface current variability is essential for advancing physical oceanography and supporting effective coastal and marine resource management in Indonesia. (Alifdini *et al.,* 2021).

At the regional scale, ocean circulation along the southern margin of the Indonesian archipelago is primarily governed by the interaction between the South Java Current (SJC) and the Indonesian Throughflow (ITF), both of which exhibit pronounced seasonal variability. During the Northwest Monsoon (NWM), prevailing northwesterly winds drive the eastward-flowing SJC along the southern coasts of Java and the Lesser Sunda Islands, supported by wind-driven Ekman transport and coastally trapped Kelvin waves (Sprintall *et al*., 2010; Wijaya *et al.,* 2024). In contrast, during the Southeast Monsoon (SEM), southeasterly winds intensify the Pacific–Indian Ocean sea level pressure gradient, strengthening the ITF transport toward the Indian Ocean and weakening the SJC (Potemra *et al.,* 2016; Susanto *et al.,* 2012). The ITF represents the net transport of upper-ocean waters from the Pacific to the Indian Ocean through the Indonesian seas, with its surface expression south of Indonesia exhibiting seasonally varying westward to southwestward components, depending on location and monsoon phase (Sprintall *et al.,* 2014). These large-scale circulation systems collectively shape the seasonal current regimes along southern Indonesia.

At finer spatial scales, however, local circulation patterns may deviate substantially from regional flow structures due to the influence of coastal geometry, bathymetry, tidal forcing, and localized wind effects. Semi-enclosed bays along the southern coast of Sumbawa Island, such as Cempi Bay, are particularly sensitive to

https://ejournal2.undip.ac.id/index.php/ijoce
DOI: 10.14710/ijoce.v8i1.28865
Diterima/Received : 05-08-2025
Disetujui/Accepted : 14-01-2026

 ISSN: 2714-8726

the interplay between tidal currents and residual (non-tidal) circulation driven by monsoonal winds and offshore forcing. Despite its proximity to major ITF pathways, including the Sape and Sumba Straits, scientific investigations specifically addressing surface current variability within Cempi Bay remain limited. Existing studies in neighboring regions have largely focused on straits and open coastal waters, leaving a knowledge gap regarding how regional circulation signals are transformed within semi-enclosed bay systems.

To address this gap, the present study investigates the seasonal variability of surface currents in Cempi Bay by integrating in-situ Acoustic Doppler Current Profiler (ADCP) observations with surface current data derived from the Hybrid Coordinate Ocean Model (HYCOM). Recent scientific advancements have highlighted the significance of local oceanographic features, such as the South Java Current (SJC) and Indonesian Throughflow (ITF), influenced by Southeast Asian monsoon system in driving water circulation around the study location (Potemra *et al.,* 2016; Sprintall *et al.,* 2014). The seasonal variability of surface geostrophic velocity indicates the eastward current dominates the northern part of the Sumba Strait, while the small portion in the southern section is dominated by the westward flow (Bayhaqi *et al.,* 2019). However, on a local scale, as in the Cempi Bay area, the winds may significantly influence the surface current. The winds in the NWM tend to drive the surface current to the East, joining the eastward SJC while the sea level gradient between the Pacific and Indian Oceans is weakened, reducing the ITF's transport. Conversely, in SEM winds are reducing the eastward surface current to the west and strengthening the influence of the ITF by increasing the Pacific – Indian Oceans Sea level gradient (Fritz *et al.,* 2023; Potemra *et al.,* 2016).

This study aims to: (1) quantify the relative contributions of tidal and residual currents in Cempi Bay during the Northwest and Southeast Monsoons using harmonic analysis of ADCP measurements; (2) examine the seasonal differences in surface current characteristics between the eastern and western inner bay; and (3) assess the capability of HYCOM reanalysis data to represent the spatial distribution of surface currents in the vicinity of a semi-enclosed bay system.

MATERIALS AND METHODS

Cempi Bay is located on the southern coast of Sumbawa Island, Indonesia, within the influence of the Indo-Pacific oceanographic system. The bay is subject to seasonal monsoonal forcing and is located near key oceanic pathways, making it a strategic location to study current dynamics in a semi-enclosed coastal setting. Bathymetric features and coastline orientation contribute to the complexity of current circulation, especially during monsoonal transitions.

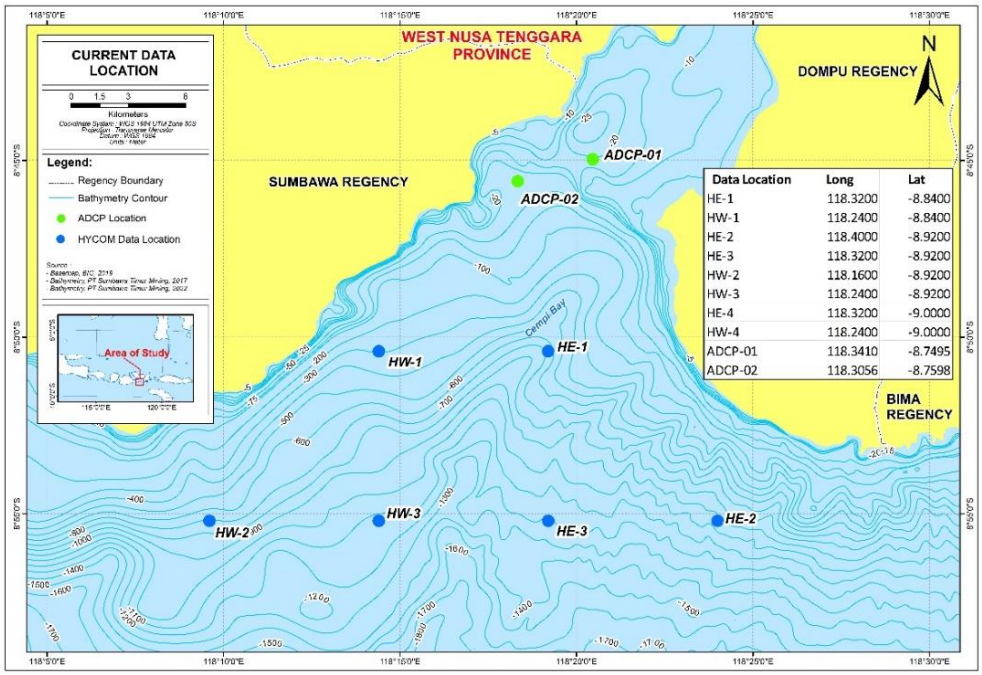

Figure 1. Surface Current Data Locations

 ISSN: 2714-8726

In-situ data

In-situ measurements using Acoustic Doppler Current Profilers (ADCPs) have been instrumental in investigating dynamic oceanic processes by providing high-resolution temporal and spatial data on current velocities and insights into the vertical structure of ocean currents. In order to measure zonal ($\bar{u}$) and meridional ($\bar{v}$) velocities, the ADCP can be installed as seabed mounted and upward looking (Cowley *et al.,* 2009; Fritz *et al.,* 2023).

ADCP is effective and efficient for long-term observations, and is able to measure with a short time interval of around 3 seconds at a water depth of 30 – 35 m (Indrayanti *et al*., 2020) when combined with historical records, the ADCP measurements provide the best coverage in various seasons, allowing for an investigation of the study area's seasonal variations (Wang *et al.,* 2022).

The seabed-mounted ADCP in this study was installed upward-looking at two fixed locations using Trawl Resistant Bottom Mounts (TRBM) system. The ADCP-01 was deployed at a total depth of ~20 m, and ADCP-02 was deployed at a total depth of ~37 m. ADCP-01 station essentially represents the eastern inner bay while ADCP-02 represents the western inner bay. Ocean current measurements include current speed and current direction. The vertical profiles setting is at 1 m vertical bin intervals, with data sampling being averaged to 20 min intervals. The current data were sampled for February 2023 to represent NWM, while data within August 2023 represent SEM. The surface current data were referenced to the local time (WITA) and ~2 m depth located at bin 19 (ADCP-01) and bin 36 (ADCP-02). After the measurement period, the ADCP was retrieved, and the data were then downloaded. The overlapping data availability from both ADCP locations is from January 31 to February 19 for NWM and from August 1 to 22 for SEM. Current data are vector quantities that are generally presented in the form of current speed (V) and direction (θ). However, the output of ADCP is also recorded in the form of north ($\bar{v}$) and east ($\bar{u}$) components.

HYCOM Global Model data

Oceanographic models such as the HYCOM have been created to supplement observational data. By combining isopycnal, sigma, and z-level coordinates, HYCOM's hybrid vertical coordinate system enables precise simulation of ocean dynamics at different depths and geographical locations (Yan & Zhu, 2023). When compared to observational data, its datasets have proven adept at reproducing upper-ocean dynamics, such as the tropical Indian Ocean's intraseasonal fluctuations in sea surface temperature and currents (Chen *et al*., 2017).

The HYCOM data used in this study are from Global Ocean Forecasting System (GOFS) 3.1 dataset with a 0.08° longitude – 0.04° latitude grid size and 41 vertical layers (Hycom.org). Surface layer data from HYCOM in this study, corresponding to the top ocean layer (2 m), were extracted at the grid point closest to the ADCP data location. Several studies are evaluating HYCOM data to investigate ocean circulation in Indonesia. Global HYCOM data are able to realistically simulate ITF seasonal variations compared with INSTANT moorings (Shinoda *et al.*, 2012). Ningsih *et al.* (2021) reveals that HYCOM current data have a good correlation with observation data (RAMA mooring and OSCAR data) in the southeastern Indian Ocean. The correlation ranges from 0.40 to 0.65, with RMSE between 0.10 and 0.29 m/s. HYCOM grid points were selected and categorized as HW-1 to HW-3 (western sector) and HE-1 to HE-3 (eastern sector) relative to the Cempi Bay axis, representing offshore locations west and east of the bay mouth, respectively, to capture spatial gradients in regional surface circulation.

Data Processing

The components of $\bar{v}$ and $\bar{u}$ from ADCP data are widely used for harmonic analysis (Sukarno and Yusuf, 2013; Respati *et al*., 2018). Each component is then used to obtain the tidal current and its harmonic constituents using the Least Squares equation (1).

$$h(t) = h_0 + \sum_{i=1}^{m} f_i H_i \cos(\omega_i t + u_i - k_i) \qquad (1)$$

where $h(t)$ = water level at time t, h_0 = mean water level, f_i = reduction factor H for the i-th constituent, H_i = mean amplitude for the i-th constituent over a lunar cycle (18.6 years), ω_i = angular velocity of the i-th constituent (2π/Ti) where Ti is the period of the i-th constituent (in hours), u_i = local equilibrium phase for the i-th constituent, κ_i = phase lag of the i-th constituent to u_i, and m = number of constituents (Boon and Kiley, 1978; Schureman, 1958; Siagian *et al*., 2021).

 ISSN: 2714-8726

The calculations for ADCP data were done in the UTide Python package. UTide is widely used for harmonic analysis and prediction of tides and tidal currents, based on the Unified Tidal Analysis and Prediction method by David Codiga (2011). From this calculation, the residual/non-tidal current (residual) can be obtained by comparing the total measured current with the tidal current from the harmonic analysis. The two components of tidal current and residual can then be displayed in the form of total velocity (Vt) and direction (θ) using equations (2) and (3) (Parker, 2007; Respati *et al*., 2018; Indrayanti *et al.,* 2021). Where $\bar{u}$ represent zonal velocity component and v for meridional velocity component.

$$V_t = \sqrt{\bar{v}^2 + \bar{u}^2} \quad (2)$$

$$\theta_t = \arctan\left(\frac{\bar{u}}{\bar{v}}\right) \quad (3)$$

The Global HYCOM data used in this study are also in $\bar{v}$ and $\bar{u}$ components of ocean currents in netCDF file format. The 3-hourly interval data was then plotted into the current rose diagram at the same data range as ADCPs to represent NWM and SEM. For the spatial distribution of surface currents, the 3-hourly data was then processed into monthly averages by using *Climate Data Operator (CDO)* and visualized by using Panoply. CDO is a set of several operators for routinely processing data from climate and forecast models, including basic arithmetic and statistical operations, tools for data selection and subsampling, and geographical interpolation. CDO typically handles NetCDF and GRIB datasets using the same set of functions in a single package (Schulzweida, 2023). The peak of the Northwest Monsoon (NWM) was defined as February 2023, while the peak of the Southeast Monsoon (SEM) was defined as August–September 2023, following established monsoonal climatology for the southern Indonesian seas.

RESULTS AND DISCUSSION

Current Characteristics on ADCP Station

The harmonic analysis performed on ADCP data at Stations ADCP-01 and ADCP-02 reveals distinct contributions and magnitudes of tidal and residual (non-tidal) currents during the Northwest Monsoon (NWM) and Southeast Monsoon (SEM) seasons (Table 1). During the NWM, the surface currents at ADCP-01 were predominantly influenced by tidal currents, which contributed 76.83% to the total current magnitude with the $\bar{v}$ and $\bar{u}$ components contributing 76.31% and 77.26%, respectively. The remaining 23.17% was attributed to residual currents. The maximum recorded current speed at this station during NWM reached 0.345 m/s, with average tidal and residual current speeds of 0.111 m/s and 0.063 m/s, respectively. Based on the time series and vector plot during the NWM, currents at ADCP-01 (Figure 2a) are also mainly influenced by tides. It was pronounced that the tidal current closely follows the total current pattern, with regular peaks showing a semi-diurnal pattern. The vectors are showing larger and more coherent tidal and total current vectors. This is supported by the harmonic analysis result, where tidal currents contribute 76.83% to the total current energy (Table 1). The residual component remains low and stable throughout this season.

The results in NWM indicate that tidal currents generally dominate the surface flow at both stations, despite the fact that the residual current at ADCP-02 is a little exceptional. The strong tidal dominance aligns with characteristics of Indonesian coastal systems, where tides often represent the majority of current energy. These results observed align well with previous studies conducted in coastal systems along the Indian Ocean facing coasts of Java, Bali, and the Lesser Sunda Islands, where tidal currents are the dominant energy driver. For instance, a detailed ADCP-based study by Syamsudin and Kaneko (2013) along the southern coast of Java and the Lesser Sunda Islands revealed that tidal currents overwhelmingly dictated current variability, while residual currents, though weaker, were present due to nonlinear tidal–topography interactions. Similarly, more localized research in Benoa Bay, Bali, by Al Tanto *et al*. (2017) used ADCP data to show that tidal currents dominated the flow in the bay (reaching up to ~1.7 m/s). This is also confirmed by Siji and Pattiaratchi (2025) in the Sape Strait and Brammadi (2024) in the Alas Strait, which are relatively close to the study area, documenting that tidal current dominance outweighs residual flow with peak speeds up to 2.5 m/s and 1.74 m/s, respectively, during spring tides. It is crucial to understand that tidal currents are the primary force behind the bay's hydrodynamics, particularly in the semi-enclosed bay. As a result, the tidal currents have a big impact on the bay's natural environment, and the dispersion and distribution of the seawater physical and chemical content (Xu *et al.,* 2023).

 ISSN: 2714-8726

The harmonic analysis during the SEM for both stations showed a more balanced contribution between tidal and residual currents. At ADCP-01, tidal currents still dominated, with a 59.76% contribution. The residual currents accounted for 40.13%. Both zonal (61.26%) and meridional (58.63%) tidal currents are also dominant. The maximum total current speed observed was 0.453 m/s, and the average tidal and residual speeds were 0.123 m/s and 0.094 m/s, respectively. Based on time series plot in the SEM (Figure 3a), the residual current at ADCP-01 becomes more variable and increases in strength, especially around early August, resulting in the tidal contribution decreasing to 59.76%, while the residual component rises to 40.13%.

Subsequently, tidal currents at ADCP-02 were also slightly dominant (59.03%) over residual currents (40.98%) during SEM. However, this station recorded the highest maximum total current speed among all observations, reaching 0.802 m/s, with a tidal maximum of 0.380 m/s and a residual maximum of 0.584 m/s. The average speeds were comparable between the two components: 0.119 m/s (tidal) and 0.098 m/s (residual), resulting in a total average current speed of 0.151 m/s. Refer to the time series plot; both tidal and residual currents show high variability (Figure 3b). However, the tidal signal still dominates and is more correlated with the total current pattern. Notable results about the u component, it exhibited a pronounced dominant residual currents (71.13%) as in NWM, while the v component remained strongly tidal (71.60%) and slightly outweighed the residual currents in SEM. Both ADCP-01 and ADCP-02 during SEM (Figure 3a & 3b) show larger aligned tidal and total current vectors, whereas the residual vectors are smaller, variably directed, and make limited contributions to the total current, reflecting the dominance of tidal currents. A pronounced difference in total current patterns is at ADCP-01, which shows a relatively balanced northeast-southwest current distribution, while ADCP-02's currents predominantly northwards or enter the bay.

The residual current at station ADCP-02 consistently exhibits greater magnitude in the zonal (east–west) direction than in the meridional (north–south) direction, indicating that the dominant forcing mechanisms are oriented along the zonal axis. This pattern reflects the influence of large-scale atmospheric and oceanographic drivers, particularly the seasonal monsoon system. During the SEM, prevailing winds originate from the southeast, whereas during the NWM, they reverse and blow from the northwest. These seasonal wind shifts are known to enhance zonal surface currents in Indonesian coastal waters. Potemra *et al*. (2016) describe this dynamic explicitly, noting that the reversal of monsoonal winds modulates the structure and intensity of regional currents, including the SJC and the ITF, both of which exhibit strong zonal orientation along the southern margin of the archipelago.

Table 1. Tidal Current Analysis at ADCP-01 and ADCP-02 Stations

Season	Result	ADCP-01			ADCP-02		
		Tidal current	Residual current	Total current	Tidal current	Residual current	Total current
NWM	Contribution (%)	76.83*	23.17	100	47.68	52.30*	100
	$\bar{u}$ (%)	76.31*	23.70	100	34.76	65.22*	100
	$\bar{v}$ (%)	77.26*	22.72	100	57.99*	42.01	100
	Max (m/s)	0.275	0.216	0.345	0.334	0.375	0.432
	Avg (m/s)	0.111	0.063	0.128	0.069	0.076	0.099
	Min (m/s)	0.001	0.003	0.004	0.002	0.005	0.004
SEM	Contribution (%)	59.76*	40.13	100	59.03*	40.98	100
	$\bar{u}$ (%)	61.26*	38.74	100	28.96	71.13*	100
	$\bar{v}$ (%)	58.63*	41.34	100	71.60*	28.37	100
	Max (m/s)	0.318	0.392	0.453	0.380	0.584	0.802
	Avg (m/s)	0.123	0.094	0.158	0.119	0.098	0.151
	Min (m/s)	0.003	0.007	0.008	0.004	0.004	0.008

Notes: *: Dominant current; NWM: Northwest Monsoon; SEM: Southeast Monsoon

 ISSN: 2714-8726

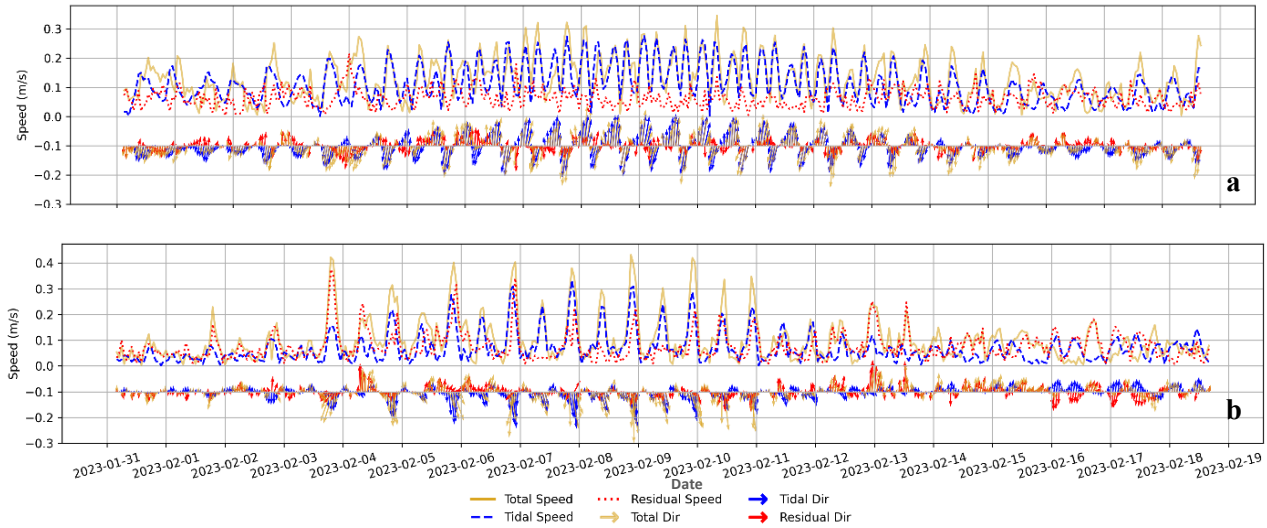

Figure 2. Time Series Current Speed and Vector Direction at (a) ADCP-01 and (b) ADCP-02 during NWM.

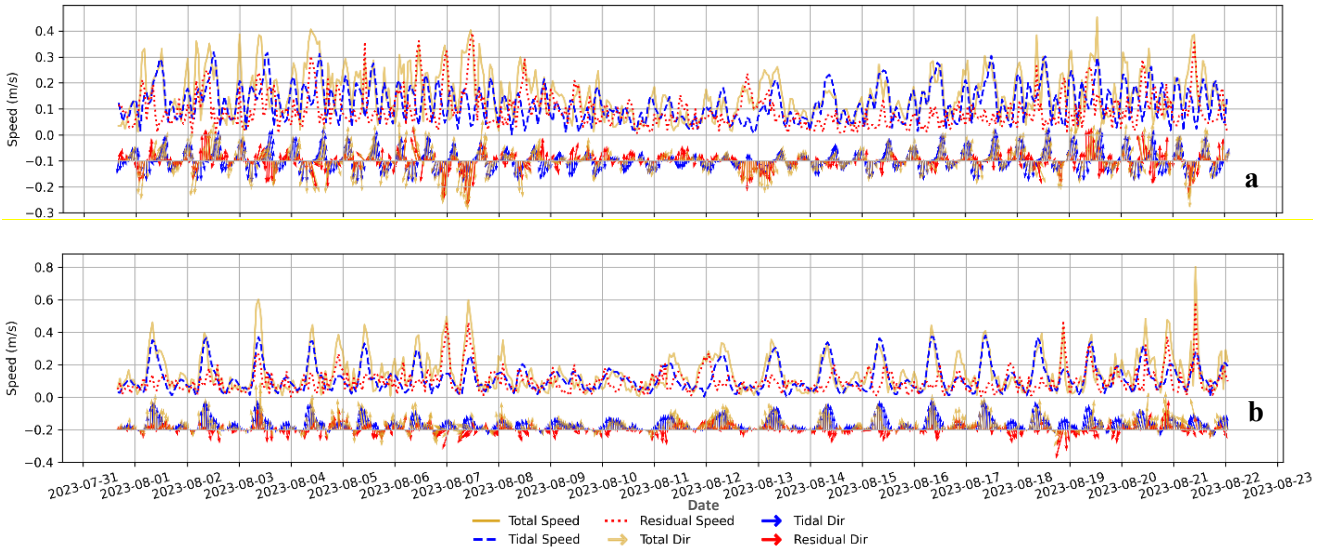

Figure 3. Time Series Current Speed and Vector Direction at (a) ADCP-01 and (b) ADCP-02 during SEM.

The prominence of zonal residual flow is further explained by the fact that ADCP-02 is located in an almost unsheltered area (Figure 1). In contrast to ADCP-01, which is located within the inner bay and is topographically sheltered by a contour bank, ADCP-02 is more directly exposed to offshore forcing. This differential exposure affects the residual flow characteristics: ADCP-02 is more susceptible to wind-driven and large-scale current influences, resulting in a clearer and stronger residual signal. Observational studies in similar geomorphological settings have shown comparable patterns. For example, Xu *et al.* (2023) reported that residual flows near bay entrances tend to be more organized and directional, while flow patterns within inner bays are typically weaker and more variable due to reduced exposure. Likewise, Hosokawa and Okura (2022) observed that tidal currents dominated the flow at the bay entrance, but residual currents associated with estuarine circulation followed topographic pathways shaped by the seabed topography. These findings reinforce the view that the enhanced zonal residual currents at ADCP-02 are not only seasonally driven but also shaped by its relatively exposed topographic position.

Currents Distribution based on ADCP and HYCOM data

The juxtaposition of ADCP measurements and HYCOM data is provided in this section to demonstrate a broader spatial and seasonal context of current patterns in the study area. This comparison is not intended as direct validation due to differences in data resolution, temporal coverage, and model assumptions. While

 ISSN: 2714-8726

ADCP data offers high-resolution in-situ observations at specific near-shore locations, the HYCOM reanalysis dataset facilitates an understanding of regional-scale circulation dynamics across the wider offshore domain. Therefore, the comparison serves to illustrate the spatial distribution and seasonal variability of ocean currents, highlighting localized versus basin-scale processes during the NWM and SEM periods.

The rose plots derived from both ADCPs and HYCOM data from the same data range reveal distinct seasonal variations in current direction and magnitude across Cempi Bay, which are shaped by the bay's morphology, monsoonal winds, and regional oceanographic features including SJC and ITF. During NWM (figure 4a), ADCP-01, located within the inner bay, exhibited a predominantly southwestward followed by northeastward flow. Despite the observed predominant southwestward flow attributed to the superposition of residual currents and water mass withdrawal during the ebb period (Figure 2a), this finding highlights the prevalence of reciprocating motion. This is particularly notable given that harmonic analysis indicates the area is strongly influenced by tidal dynamics (76.83%).

Conversely, ADCP-02, located marginally closer to the bay opening yet within the inner zone, registered a more dispersed current pattern. The rose diagram shows predominantly oriented northeastward, followed by southeastward. With the fact that this station has slightly stronger residual currents (52.30%; Table 1), indicating potential influence from regional residual flows driven by monsoonal winds. Notably, currents are directed towards the southeast. As the predominant current in this station is northeastward, this demonstrates a circulation pattern where, in this season, seawater primarily enters the bay from the west side (ADCP-02) and exits from the east side (ADCP-01).

The current roses at the bay mouth stations (HW-1 and HE-1) reveal predominantly eastward to southeastward flow patterns with more occurrence towards the other directions. These transition zones at the bay mouth are influenced by a mix of semi-enclosed bay dynamics and oceanic forcing. The HYCOM current roses at these locations support the presence of enhanced directional variability, which may reflect the interplay between local wind stress, tidal interactions, and oceanic inflow, including contributions from large-scale regional circulation. At farther offshore stations (HW-2, HW-3, HE-2, and HE-3), the NWM current roses exhibit consistent eastward to southeastward directions, suggesting a stronger influence of large-scale regional circulation patterns. These currents align with the SJC, which during the NWM transports surface waters eastward along the southern margin of the Lesser Sunda Islands, driven by northwest monsoonal wind forcing (Potemra *et al.,* 2016; Syamsudin and Kaneko, 2013; Utari *et al.,* 2019).

In contrast, during the SEM, the current dynamics at ADCP-01 exhibited a notable shift, with flow directions alternating between northeastward and southwestward. This bidirectional behavior likely reflects a tidal dominance pattern. However, the stronger northeastward current shows more immediate and dynamic response to prevailing monsoonal wind forcing and the strengthening ITF, despite the station's location within the relatively sheltered inner bay. At ADCP-02, a distinct pattern emerged, where the currents became strongly, almost unidirectional toward the north and demonstrated a marked intensification in magnitude. The maximum observed velocity at this station reached 0.802 m/s, representing the highest recorded speeds. The current rose diagrams further illustrate that during high tide, the inflow into the bay is composed of both tidal and residual current components. Conversely, during low tide, the ebbing tidal current is opposed by a residual current that persistently flows into the bay, resulting in a partial cancellation of flow energy. This interaction indicates that, although tidal currents remain dominant during this season, there is a noticeable increase in residual current influence. These findings are consistent with the harmonic analysis discussed in the preceding section (Table 1).

The shift in current orientation at HE-1 and HW-1 became more variable, predominantly westward or southwestward. Subsequently across most offshore stations, becoming more unidirectional, exhibited consistent westward currents at HW-2, HW-3, HE-2, and HE-3, directly reflecting the dominant ITF pathway during this season. This seasonal reversal is consistent with the southeast monsoonal wind pattern, which dominates from July to September, reversing the direction of regional surface flows (Pang *et al.,* 2021; R. Susanto *et al*., 2012). This alignment corresponds with the intensified ITF during the SEM, when the pressure gradient between the Pacific and Indian Oceans achieves its strongest (Pang *et al.,* 2021; Potemra *et al.,* 2016). The interplay between monsoonal winds, tidal modulation, and ITF advection creates a spatial gradient of current dynamics from inner to outer Cempi Bay. Inner bay stations are predominantly governed by local tidal currents. In contrast, the bay mouth functions as a transitional zone, while offshore regions experience a progressively increasing influence from the regional ITF system.

 ISSN: 2714-8726

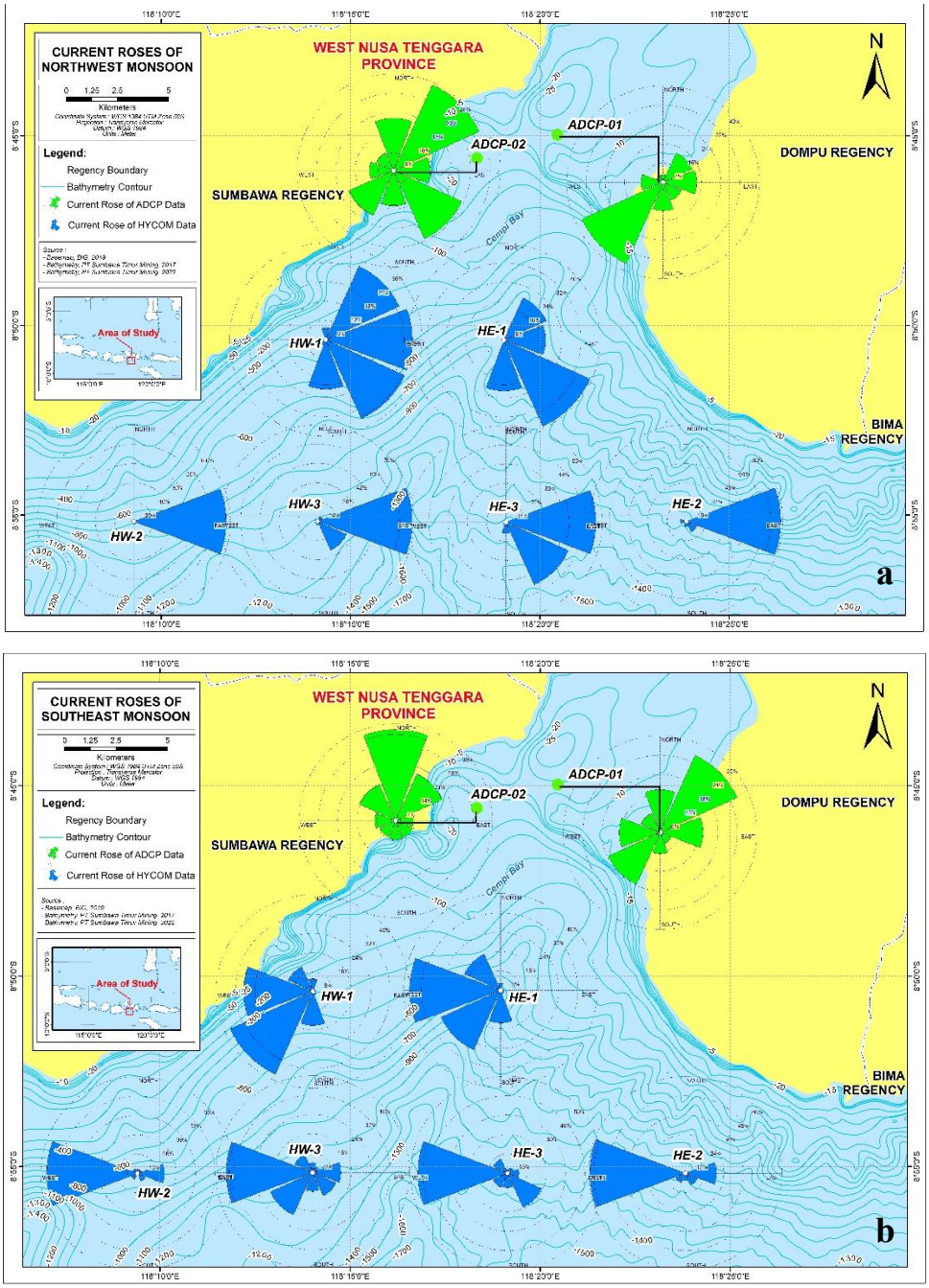

Figure 4. Current Rose Diagram at ADCPs and HYCOM data locations during NWM and SEM

In contrast, the southern coast of Sumbawa, including Cempi Bay, experiences weaker eastward currents, as the influence of the broader monsoonal circulation diminishes closer to shore. The Sumba Strait, located to the south of Sumbawa and north of Sumba Island, also exhibits moderate eastward currents during this period, contributing to the overall eastward transport of water masses. This behavior is influenced by the eastward extension of the SJC, which can reach as far as the Ombai Strait of boreal winter driven by both the wind-driven Ekman flow during the northwest monsoon and the strongest semi-annual Kelvin waves (Bayhaqi *et al*., 2019; Sprintall *et al*., 2010). The strengthening of the SJC, driven by northwesterly monsoonal winds and associated sea level gradients, enhances the advection of surface waters from the Java Sea and southern Makassar Strait eastward along the southern coasts of the Lesser Sunda Islands, including Cempi bay

 ISSN: 2714-8726

waters. This linkage suggests that the observed surface flows in the Sumba Strait are not solely locally generated but are also dynamically connected to the broader SJC circulation system (Iskandar *et al*., 2005; Susanto *et al*., 2012; Syamsudin & Kaneko, 2013).

As the monsoon shifts to the SEM phase (Figure 5b), it reveals a marked intensification of surface flow, particularly in the Lombok Strait, Sape, and Sumba Straits and extending southward into the Savu and Indian Seas. Surface velocities exceed 1.0 m/s and reach up to ~1.9 m/s, signifying a strongly enhanced ITF pathway. The enhanced southwestward transport is a direct consequence of the elevated Pacific–Indian Ocean pressure gradient during the southeast monsoon, observed in July to September, and aligns with established ITF, resulting in the weakening of SJC (Ningsih *et al*., 2021; Potemra *et al*., 2016; Susanto *et al*., 2021). In addition, the Lombok and Sape Straits display coherent of enhanced southwestward transport toward the Indian Ocean, further evidencing the monsoon-modulated routing of ITF and its role in driving regional circulation patterns. These observations align with satellite drifter and altimetry-based studies by Siji & Pattiaratchi (2025) that report similar current amplification and directional consistency through these straits during the southeast season.

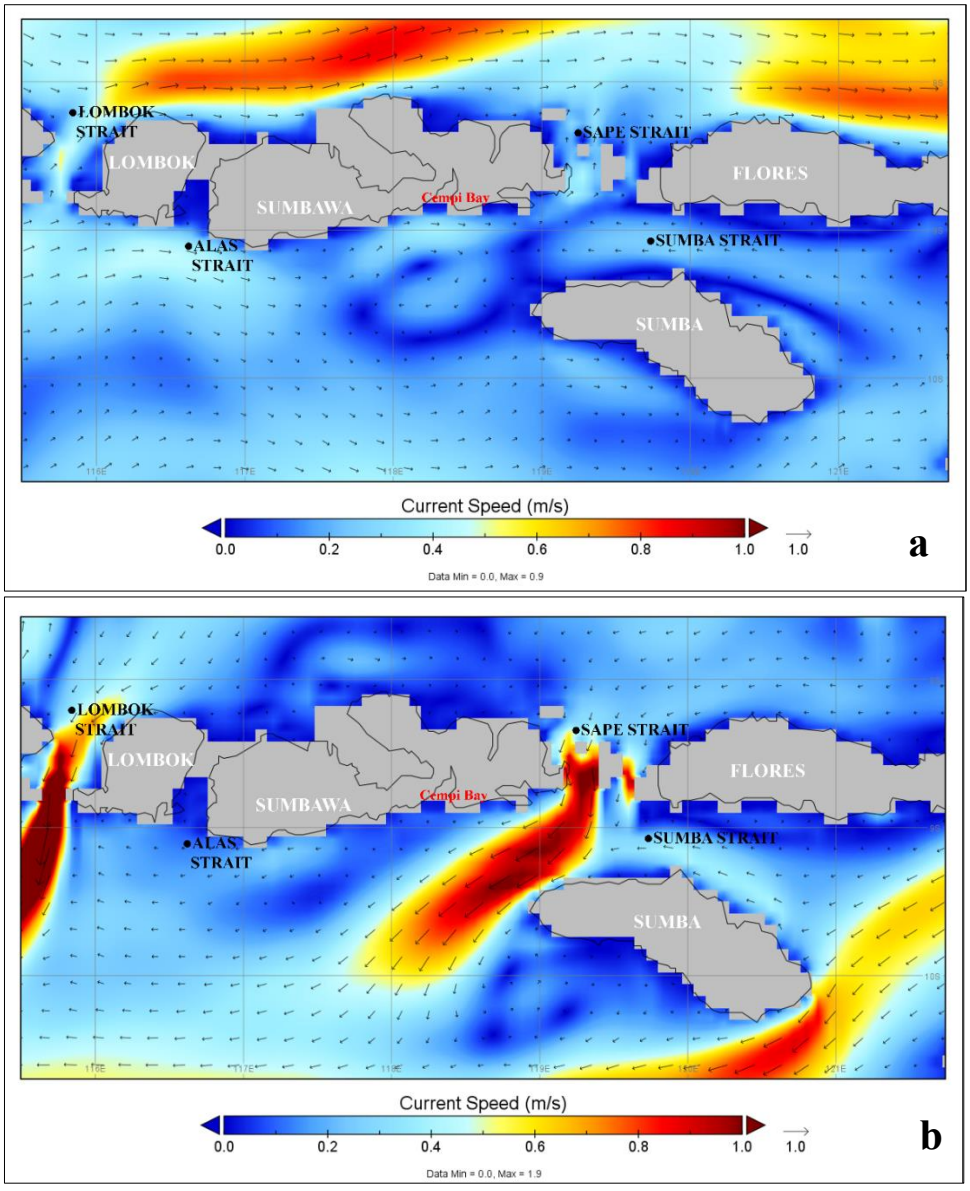

Figure 5. Surface Current Speed at the study area during (a) NWM; 31 January–19 February 2023, (b) SEM; 1–22 August 2023

 ISSN: 2714-8726

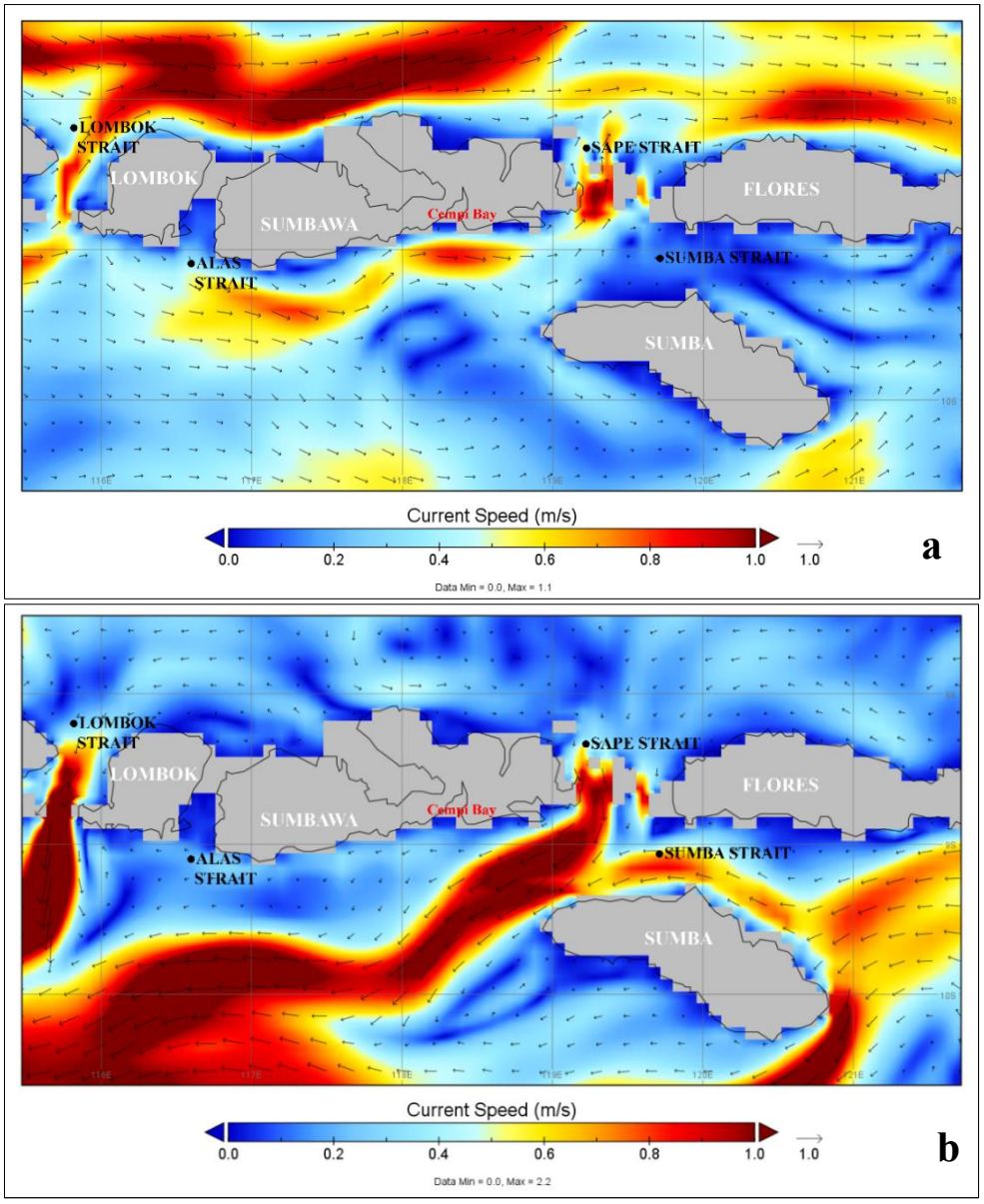

Figure 6. Surface Current Speed at the study area during (a) Peak of NWM, and (b) Peak of SEM.

The peak of SEM (Figure 6b) is characterized by strong westward surface currents, particularly south of Sumbawa and Lombok, where the Sape and Sumba Straits become a major pathway for westward flow contribution to the Cempi Bay and eventually toward the Indian Ocean. The Lombok and Sape Straits also display a reversal in current direction, with the surface water mass now moving from the Flores Sea and Banda Sea toward the Indian Ocean. In this season, Cempi Bay experiences a notable increase in current speed and a clear shift to westward flow, reflecting the intensified influence of the prevailing southeasterly winds and massive ITF transport that mostly flows through Sape Strait. As this strait is one of the key passages of ITF into the Indian Ocean besides the Sunda, Bali, Lombok, Alas, and Ombai Straits, and the Timor passage (Siji and Pattiaratchi, 2025; Susanto *et al*., 2021). The current corridor appears to extend toward the east and south of Sumba Island, hinting at a connectivity influenced by ITF that exits through the Ombai Strait (Bayhaqi *et al*., 2019; Fritz *et al*., 2023; Ningsih *et al*., 2021; Siji and Pattiaratchi, 2025).

This study presents some important findings regarding the seasonal circulation at the Cempi Bay through a combination of ADCP field data and HYCOM model output; however, several limitations should be noted. The ADCP measurements were limited to two fixed stations, which may not fully represent current variability

 ISSN: 2714-8726

of the entire bay, particularly in offshore or bay mouth areas. The study was confined to two monsoonal periods (NWM and SEM) in 2023, without covering transitional or interannual changes. HYCOM's coarse resolution and generalized bathymetry reduce its reliability near the coast, particularly in semi-enclosed bays. Tidal analysis using UTide was based on short-term data and may not fully capture nonlinear interactions. Lastly, wind data were not included, even though wind forcing likely influences residual currents, especially at the more exposed ADCP-02 site. Despite these limitations, the findings in this study offer valuable insights into the seasonal circulation characteristics of Cempi Bay and provide a foundation for more comprehensive oceanographic investigations in the future.

CONCLUSION

The results of seasonal surface current variability in Cempi Bay based on harmonic decomposition of in-situ ADCP measurements and spatial interpretation of HYCOM reanalysis data demonstrate that tidal forcing constitutes the principal driver of surface circulation within the inner bay, particularly at the eastern station (ADCP-01), where tidal contributions reached 76.83% during the Northwest Monsoon (NWM). In contrast, the western inner bay (ADCP-02) exhibited a comparatively stronger residual component, with residual currents slightly exceeding tidal contributions during NWM and remaining substantial during the Southeast Monsoon (SEM). Seasonal contrasts were evident in both magnitude and directional structure. During NWM, surface circulation was predominantly characterized by reciprocating tidal motion with limited residual influence, especially at ADCP-01. During SEM, residual currents intensified at both stations, resulting in a more balanced tidal–residual contribution (~59% tidal and ~40% residual). The highest current speeds were recorded at ADCP-02 during SEM (up to 0.802 m/s), reflecting enhanced exposure to offshore forcing and stronger monsoon-driven advection. The pronounced zonal orientation of residual currents, particularly at the more exposed western station, indicates the influence of monsoonal wind stress and regional-scale circulation pathways interacting with local bathymetry and bay geometry. The spatial analysis derived from HYCOM complements the point-based ADCP observations by illustrating the broader regional setting. The model captures the seasonal reversal of surface circulation, with eastward-dominant flow during NWM and intensified westward transport during SEM associated with strengthened throughflow pathways south of Sumbawa. Although HYCOM underestimates nearshore magnitudes due to resolution constraints and simplified bathymetry, it effectively represents the large-scale directional patterns that modulate circulation at the bay mouth and offshore sectors. Overall, the integration of high-resolution field measurements and regional model output reveals a clear spatial gradient of hydrodynamic control in Cempi Bay: tidal dominance within the sheltered inner bay, transitional dynamics near the bay mouth, and increasing influence of monsoon-modulated regional circulation offshore. These findings contribute to a more refined understanding of semi-enclosed bay hydrodynamics along the southern Indonesian margin and establish an empirical baseline for future investigations addressing interannual variability, wind–current coupling, and implications for coastal environmental management.

ACKNOWLEDGEMENT

The author would like to express sincere gratitude to all parties who contributed to the success of this research, particularly for the provision of primary data and the support granted for the publication of its findings. Appreciation is also extended to all individuals who offered assistance throughout the research process, whose contributions, although not mentioned individually, were truly valuable.

REFERENCES

Al Tanto, T., Wisha, U. J., Kusumah, G., Pranowo, W. S., Husrin, S., & Putra, A. 2017. Karakteristik Arus Laut Perairan Teluk Benoa-Bali (Characteristics of Sea Current in Benoa Bay Waters-Bali). *Jurnal Ilmiah Geomatika*, 23: 37–48.

Alifdini, I., Shimada, T., & Wirasatriya, A. 2021. Seasonal distribution and variability of surface winds in the Indonesian seas using scatterometer and reanalysis data. *International Journal of Climatology*, 41: 4825–4843. https://doi.org/10.1002/joc.7101

Bayhaqi, A., Lenn, Y.-D., Surinati, D., Polton, J., Nur, M., Corvianawatie, C., & Purwandana, A. 2019. The Variability of Indonesian Throughflow in Sumba Strait and Its Linkage to the Climate Events. *American Journal of Applied Sciences*, 16: 118–133. https://doi.org/10.3844/ajassp.2019.118.133

 ISSN: 2714-8726

Brammadi, S. 2024. Observed Bi-Directional Tidal and Southward Currents from Vessel Mounted ADCP Surveys in the Alas Strait. Institut Teknologi Bandung.

Fritz, M., Mayer, M., Haimberger, L., & Winkelbauer, S. 2023. Assessment of Indonesian Throughflow transports from ocean reanalyses with mooring-based observations. *Ocean Science*, 19: 1203–1223. https://doi.org/10.5194/os-19-1203-2023

Hosokawa, S., & Okura, S. 2022. Long-term observation of current at the mouth of Tokyo Bay. *Coastal Engineering Journal*, 64: 648–659. https://doi.org/10.1080/21664250.2022.2122300

Iskandar, I., Mardiansyah, W., Masumoto, Y., & Yamagata, T. 2005. Intraseasonal Kelvin waves along the southern coast of Sumatra and Java. *Journal of Geophysical Research: Oceans*, 110: 1–12. https://doi.org/10.1029/2004JC002508

Ningsih, N. S., Sakina, S. L., Susanto, R. D., & Hanifah, F. 2021. Simulated zonal current characteristics in the southeastern tropical Indian Ocean (SETIO). *Ocean Science*, 17: 1115–1140. https://doi.org/10.5194/os-17-1115-2021

Pang, X., Bassinot, F., & Sepulcre, S. 2021. Indonesian Throughflow variability over the last two glacial-interglacial cycles: Evidence from the eastern Indian Ocean. *Quaternary Science Reviews*, 256: 106839. https://doi.org/10.1016/j.quascirev.2021.106839

Potemra, J. T., Hacker, P. W., Melnichenko, O., & Maximenko, N. 2016. Satellite estimate of freshwater exchange between the Indonesian Seas and the Indian Ocean via the Sunda Strait. *Journal of Geophysical Research: Oceans*, 121: 5098–5111. https://doi.org/10.1002/2015JC011618

Siji, P., & Pattiaratchi, C. 2025. Surface Current Observations in the Southeastern Tropical Indian Ocean Using Drifters. *Journal of Marine Science and Engineering*, 13. https://doi.org/10.3390/jmse13040717

Sprintall, J., Gordon, A. L., Koch-Larrouy, A., Lee, T., Potemra, J. T., Pujiana, K., & Wijffels, S. E. 2014. The Indonesian seas and their role in the coupled ocean-climate system. *Nature Geoscience*, 7: 487–492. https://doi.org/10.1038/ngeo2188

Sprintall, J., Wijffels, S., Molcard, R., & Jaya, I. 2010. Direct evidence of the South Java Current system in Ombai Strait. *Dynamics of Atmospheres and Oceans*, 50: 140–156. https://doi.org/10.1016/j.dynatmoce.2010. 02.006

Sprintall, J., Wijffels, S. E., Molcard, R., & Jaya, I. 2009. Direct estimates of the Indonesian Throughflow entering the Indian Ocean: 2004–2006. *Journal of Geophysical Research: Oceans*, 114. https://doi.org/10.1029/2008JC005257

Susanto, D., Waworuntu, J., Prayogo, W., & Setianto, A. 2021. Moored Observations of Current and Temperature in the Alas Strait: Collected for Submarine Tailing Placement, Used for Calculating the Indonesian Throughflow. *Oceanography*, 34. https://doi.org/10.5670/oceanog.2021.103

Susanto, R. D., Ffield, A., Gordon, A. L., & Adi, T. R. 2012. Variability of Indonesian throughflow within Makassar Strait, 2004–2009. *Journal of Geophysical Research: Oceans*, 117. https://doi.org/10.1029/2012JC008096

Syamsudin, F., & Kaneko, A. 2013. Ocean variability along the southern coast of Java and Lesser Sunda Islands. *Journal of Oceanography*, 69: 557–570. https://doi.org/10.1007/s10872-013-0192-6

Utari, P. A., Setiabudidaya, D., Khakim, M. Y. N., & Iskandar, I. 2019. Dynamics of the South Java Coastal Current revealed by RAMA observing network. *Terrestrial, Atmospheric and Oceanic Sciences*, 30: 235–245. https://doi.org/10.3319/TAO.2018.12.14.01

Wijaya, Y. J., Wisha, U. J., Rejeki, & H. A. 2024. Variability of the South Java Current from 1993 to 2021, and its relationship to ENSO and IOD events. *Asia-Pacific Journal of Atmospheric Sciences*, 60: 65–79. https://doi.org/10.1007/s13143-023-00336-2

Xu, Y., Wang, Y., Hu, S., Zhu, Y., Zuo, J., & Zeng, J. 2023. Study on the Impact of the Coastline Changes on Hydrodynamics in Xiangshan Bay. *Applied Sciences*, 13. https://doi.org/10.3390/app13148071